

## Decomposition of A-Type Sandwiches. Synthesis and Characterization of New Polyoxometalates Incorporating Multiple d-Electron-Centered Units

Michelle D. Ritorto, Travis M. Anderson, Wade A. Neiwert, and Craig L. Hill\*

Department of Chemistry, Emory University, Atlanta, Georgia 30322

Received September 22, 2003

The controlled decomposition of the sandwich-type polyoxometalates  $K_{12}[(M(OH)_2)_3(A-\alpha-PW_9O_{34})_2]$  (where  $M = Mn(II)$  or  $Co(II)$ ) in 0.5 M NaCl yields a new family of transition metal substituted POMs of the general formula  $[(MOH_2)_2M_2PW_9O_{34}]_2(PW_6O_{26})^{17-}$  (where  $M = Mn(II)$  (**1Mn**) or  $Co(II)$  (**1Co**)). The structure of **1Mn**, determined by single-crystal X-ray diffraction ( $a = 17.4682(10)$  Å,  $b = 22.3071(12)$  Å,  $c = 35.1195(18)$  Å,  $\beta = 95.898(1)^\circ$ , monoclinic,  $P2_1/c$ ,  $Z = 4$ ,  $R_1 = 6.19\%$ , based on 50264 independent reflections), consists of two B- $\alpha$ -( $Mn^{II}OH_2$ )- $Mn^{II}_2PW_9O_{34}^{3-}$  units joined by a B-type hexavacant  $PW_6O_{26}^{11-}$  fragment to form a C-shaped polyoxometalate. A low resolution X-ray structure of the Co(II) analogue, **1Co**, was also obtained. The UV–visible spectrum of **1Co** shows the characteristic charge-transfer bands of polyoxometalates as well as a new Co-centered peak (560 nm,  $\epsilon = 416 M^{-1} cm^{-1}$ ) which appears at a higher wavelength relative to that exhibited by the parent A-type sandwich,  $K_{12}[(Co(OH)_2)_3(A-\alpha-PW_9O_{34})_2]$ . The methyltricaprylammonium salt of **1Mn** is an effective catalyst for the  $H_2O_2$ -based epoxidation of *cis*-cyclooctene, cyclohexene, and 1-hexene.

### Introduction

The versatility and accessibility of polyoxometalates (POMs) have led to many recent applications of these compounds in catalysis and molecular magnetism.<sup>1–6</sup> The framework of many POMs including heteropolytungstates consists of  $d^0$  W(VI) atoms bound to oxo ( $O^{2-}$ ) ligands which render them oxidatively resistant and hence particularly attractive as homogeneous and heterogeneous catalysts. The substitution of one or more of the skeletal W(VI) atoms with d-electron-containing transition metal cations affords oxidatively resistant catalysts, and these complexes and their catalysis have been extensively reviewed.<sup>7–14</sup>

This paper addresses the decomposition of A-type Keggin sandwich complexes originally reported by Knoth and co-workers.<sup>15,16</sup> These  $\sim D_{3h}$  structures are composed of two A- $\alpha$ - $PW_9O_{34}^{n-}$  units linked by three corner-sharing transition metal cations (formula  $[(M(OH)_2)_3(\alpha-PW_9O_{34})_2]^{n-}$ ). The A-type sandwich complexes of the divalent metals (and in particular Co(II)) are not stable in aqueous solution and quickly convert to the B-type isomers (formula  $[(MOH_2)_2-M_2(PW_9O_{34})_2]^{n-}$ ) based on UV–visible spectroscopic data.<sup>16</sup> Contant has also studied the A-type decomposition process by UV–visible spectroscopy, and he has identified a number

\* Author to whom correspondence should be addressed. E-mail: chill@emory.edu.

- (1) Pope, M. T. *Heteropoly and Isopoly Oxometalates*; Springer-Verlag: Berlin, 1983.
- (2) Topical issue on polyoxometalates: Hill, C. L., Guest Ed. *Chem. Rev.* **1998**, *98*, 1–389.
- (3) *Polyoxometalate Chemistry: From Topology via Self-Assembly to Applications*; Pope, M. T., Müller, A., Eds.; Kluwer Academic Publishers: Dordrecht, Netherlands, 2001.
- (4) *Polyoxometalate Chemistry for Nano-Composite Design*; Yamase, T., Pope, M. T., Eds.; Nanostructure Science and Technology; Kluwer Academic/Plenum Publishing: New York, 2002.
- (5) Pope, M. T. Polyoxo Anions: Synthesis and Structure. In *Comprehensive Coordination Chemistry II: Transition Metal Groups 3-6*; Wedd, A. G., Ed.; Elsevier Science: New York; Vol. 4, Chapter 3.10, in press.

- (6) Hill, C. L. Polyoxo Anions: Reactivity. In *Comprehensive Coordination Chemistry II: Transition Metal Groups 3-6*; Wedd, A. G., Ed.; Elsevier Science: New York; Vol. 4, Chapter 3.11, in press.
- (7) Hill, C. L.; Brown, R. B., Jr. *J. Am. Chem. Soc.* **1986**, *108*, 536–538.
- (8) Hill, C. L.; Prosser-McCartha, C. M. *Coord. Chem. Rev.* **1995**, *143*, 407–455.
- (9) Okuhara, T.; Mizuno, N.; Misono, M. *Adv. Catal.* **1996**, *41*, 113–252.
- (10) Mizuno, N.; Misono, M. *Chem. Rev.* **1998**, *98*, 199–218.
- (11) Kozhevnikov, I. V. *Chem. Rev.* **1998**, *98*, 171–198.
- (12) Neumann, R. *Prog. Inorg. Chem.* **1998**, *47*, 317–370.
- (13) Katsoulis, D. E. *Chem. Rev.* **1998**, *98*, 359–388.
- (14) Kozhevnikov, I. V. *Catalysis by Polyoxometalates*; Wiley: Chichester, England, 2002; Vol. 2.
- (15) Knoth, W. H.; Domaille, P. J.; Harlow, R. L. *Inorg. Chem.* **1986**, *25*, 1577–1584.
- (16) Knoth, W. H.; Domaille, P. J.; Farlee, R. D. *Organometallics* **1985**, *4*, 62–68.

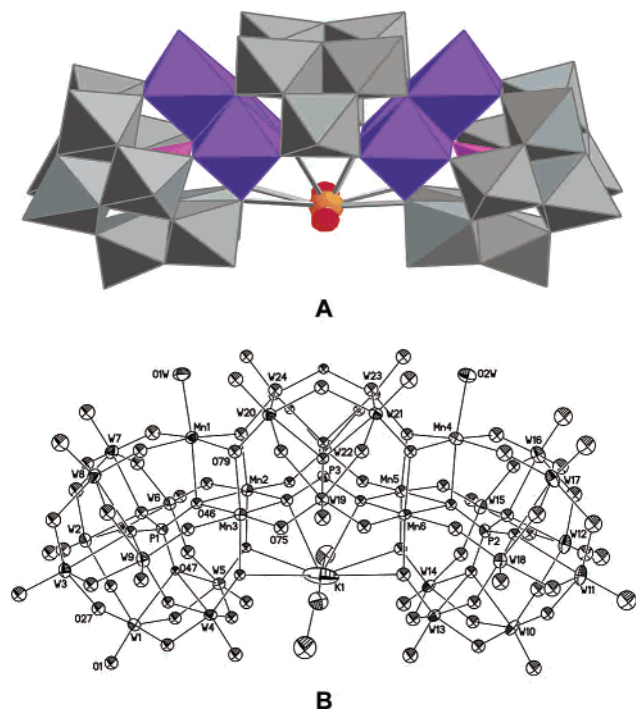


**Figure 1.** (A) Polyhedral representation of  $[(\text{Mn}^{\text{II}}\text{OH}_2)\text{Mn}^{\text{II}}\text{PW}_9\text{O}_{34}]_2(\text{PW}_6\text{O}_{26})^{17-}$  (**1Mn**). (B) Thermal ellipsoid plot (50% probability surfaces) of **1Mn**. The single  $\text{K}^+$  cation is shown in the bend of **1Mn** while the  $\text{Na}^+$  cations are omitted for clarity.

of intermediates that appear as a function of the counteranions (i.e.  $\text{Na}^+$  or  $\text{K}^+$ ) and the rotational isomerism of the POM precursor used (i.e.  $\text{A-}\alpha\text{-PW}_9\text{O}_{34}^{9-}$  versus  $\text{A-}\beta\text{-PW}_9\text{O}_{34}^{9-}$ ).<sup>17</sup> More recently, Hervé and co-workers have synthesized a Si analogue of  $[(\text{Co}(\text{OH}_2)_2)_3(\text{PW}_9\text{O}_{34})_2]^{12-}$ .<sup>18</sup> UV–visible studies of this compound show that it too decomposes in aqueous solution with two different intermediate species formed.

We now report the first reactions of the A-type sandwich complexes in 0.5 M NaCl. The results show that a new family of transition-metal substituted POMs form of the general formula  $[(\text{MOH}_2)_2\text{M}_2\text{PW}_9\text{O}_{34}]_2(\text{PW}_6\text{O}_{26})^{17-}$  (where  $\text{M} = \text{Mn}(\text{II})$  (**1Mn**) or  $\text{Co}(\text{II})$  (**1Co**); Figure 1). These compounds are characterized by X-ray crystallography, infrared and UV–visible spectroscopy, magnetism, thermogravimetric analysis (TGA), differential scanning calorimetry (DSC), and elemental analysis. In addition, preliminary catalytic studies show that **1Mn** is a selective catalyst for the  $\text{H}_2\text{O}_2$ -based epoxidation of alkenes.

## Experimental Section

**General Methods and Materials.** Elemental analyses of Co, K, Mn, Na, P, and W were performed by Kanti Labs (Mississauga, ON, Canada). Infrared spectra (2% sample in KBr) were recorded on a Nicolet 510 FT-IR spectrometer. Electronic spectra were recorded on a Hewlett-Packard 8452A diode array spectrophotometer using a 1.000-cm-optical-path quartz cuvette with 0.5 M NaCl as the solvent. Average magnetic susceptibilities were measured on a Johnson Matthey MSB-1 magnetic susceptibility balance as neat powders at 25 °C; the balance was calibrated using  $\text{Hg}[\text{Co}(\text{SCN})_4]$  as a standard. Thermogravimetric analysis and differential scanning calorimetry were performed on an Instrument Specialists

Incorporated (ISI) TGA 1000 and DSC 550, respectively.  $^{31}\text{P}$  NMR measurements were made on a Varian INOVA 400 MHz spectrometer using 85%  $\text{H}_3\text{PO}_4$  as an external reference. Organic oxidation products were quantified using a Hewlett-Packard 6890 gas chromatograph fitted with a 5% phenyl methyl silicone capillary column, a flame ionization detector, and a Hewlett-Packard 6890 series integrator (with  $\text{N}_2$  as the carrier gas).

**Synthesis of  $[(\text{MOH}_2)_2\text{M}_2\text{PW}_9\text{O}_{34}]_2(\text{PW}_6\text{O}_{26})^{17-}$  (**1**).**  $\text{K}_{12}[(\text{M}(\text{OH}_2)_2)_3(\text{A-}\alpha\text{-PW}_9\text{O}_{34})_2]$  (where  $\text{M} = \text{Mn}(\text{II})$  or  $\text{Co}(\text{II})$ ) was prepared and purified by the literature method, and purity was confirmed by FT-IR and elemental analysis.<sup>15,16</sup> For the Mn complex, **1Mn**, the purified  $\text{K}_{12}[(\text{Mn}(\text{OH}_2)_2)_3(\text{A-}\alpha\text{-PW}_9\text{O}_{34})_2]$  (0.200 g) was dissolved in a minimal amount of 0.5 M NaCl. Gold, rod-shaped crystals formed upon slow evaporation. The isolated yield based on Mn = 30%. IR (2% KBr pellet 1150–675  $\text{cm}^{-1}$ ): 1060 (w, sh), 1043 (s), 1022 (s), 953 (m, sh), 931 (s), 893 (w, sh), 880 (s), 823 (w, sh), 791 (m), 729 (s). Magnetic susceptibility:  $\mu_{\text{eff}} = 11.68 \mu_{\text{B}}/\text{mol}$  at 298 K. Anal. Calcd for  $\text{K}_{4.75}\text{Na}_{12.25}\text{Mn}_6\text{P}_3\text{W}_{24}\text{O}_{108}\text{H}_{28}$ : K 2.63, Na 3.99, Mn 4.67, P 1.32, W 62.51. Found: K 2.69, Na 3.93, Mn 4.65, P 1.32, W 62.51. [MW = 7062 g/mol.]

The Co analogue was prepared similarly using the appropriate A-type sandwich as a precursor. Magenta, needle-shaped crystals formed upon slow evaporation. The isolated yield based on Co = 56%. IR (2% KBr pellet 1150–675  $\text{cm}^{-1}$ ): 1087 (m, sh), 1033 (s), 955 (m, sh), 935 (s), 887 (s), 786 (w), 727 (s). Magnetic susceptibility:  $\mu_{\text{eff}} = 12.69 \mu_{\text{B}}/\text{mol}$  at 298 K. Anal. Calcd for  $\text{K}_5\text{Na}_{12}\text{Co}_6\text{P}_3\text{W}_{24}\text{O}_{108}\text{H}_{28}$ : K 2.76, Na 3.89, Co 4.99, P 1.31, W 62.26. Found: K 2.79, Na 3.85, Co 4.93, P 1.40, W 63.15. [MW = 7086 g/mol.]

**X-ray Crystallography.** A suitable crystal of **1Mn** was coated with Paratone N oil, suspended on a small fiber loop, and placed in a stream of cooled nitrogen (173 K) on a Bruker D8 SMART APEX CCD sealed tube diffractometer with graphite monochromated Mo  $\text{K}\alpha$  (0.71073 Å) radiation. A sphere of data was measured using combinations of  $\phi$  and  $\omega$  scans with 10 s frame exposures and 0.3° frame widths. Data collection, indexing, and initial cell refinements were carried out using SMART software.<sup>19</sup> Frame integration and final cell refinements were carried out using SAINT software.<sup>20</sup> Final cell parameters were determined from least-squares refinement. The crystal faces were indexed and absorption corrections were made in XPREP.<sup>21</sup> Additionally, a multiple absorption correction for each data set was applied using the program SADABS.<sup>22</sup> The structure was determined using direct methods and difference Fourier techniques.<sup>21</sup> The largest residual electron density was located less than 1.0 Å from the W addenda atoms and was most likely due to an imperfect absorption correction often encountered in heavy-metal atom structures. All K, Na, Mn, P, and W atoms were refined using anisotropic thermal parameters except for Na18, Na20, and Na22. Most of the O atoms of the waters of hydration were also refined anisotropically except for O8w, and O24w–O56w. The O atoms of the POM were refined using isotropic thermal parameters. Many of the Na and solvent water O atoms were disordered and were refined with partial occupancies based on their high thermal parameters (see Supporting Information, SI). No H atoms associated with the water molecules were located in the difference Fourier map. The final R1 scattering

(17) Contant, R. *Can. J. Chem.* **1987**, *65*, 568–573.

(18) Laronze, N.; Marrot, J.; Hervé, G. *Inorg. Chem.* **2003**, *42*, 5857–5862.

(19) SMART, version 5.624; Bruker AXS, Inc.: Madison, WI, 2002.

(20) SAINT, version 6.36A; Bruker AXS, Inc.: Madison, WI, 2002.

(21) SHELXTL, version 6.12; Bruker AXS, Inc.: Madison, WI, 2002.

(22) Sheldrick, G. SADABS, version 2.03; University of Göttingen: Göttingen, Germany, 2001.

**Table 1.** Crystallographic Data and Structure Refinement for **1Mn**

empirical formula	H <sub>84</sub> KMn <sub>6</sub> Na <sub>16</sub> O <sub>136</sub> P <sub>3</sub> W <sub>24</sub>
formula weight	7502.56
space group	<i>P</i> 2 <sub>1</sub> / <i>c</i> (No. 14)
unit cell	<i>a</i> = 17.4682(10) Å <i>b</i> = 22.3071(12) Å <i>c</i> = 35.1195(18) Å <i>β</i> = 95.898(1)°
volume	13626.4(13) Å <sup>3</sup>
<i>Z</i>	4
density (calcd)	3.657 g cm <sup>-3</sup>
temperature	-100(2) °C
<i>λ</i>	0.71073 Å
<i>μ</i>	2.0934 cm <sup>-1</sup>
GOF	1.009
final <i>R</i> <sub>1</sub> <sup>a</sup> [ <i>I</i> > 2σ( <i>I</i> )]	0.0619
final w <i>R</i> <sub>2</sub> <sup>b</sup> [ <i>I</i> > 2σ( <i>I</i> )]	0.1008

$$^a R_1 = \sum ||F_o| - |F_c|| / \sum |F_o|, \quad ^b wR_2 = \{ \sum [w(F_o^2 - F_c^2)^2] / \sum [w(F_o^2)^2] \}^{0.5}$$

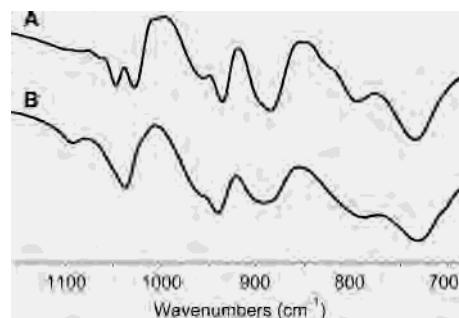
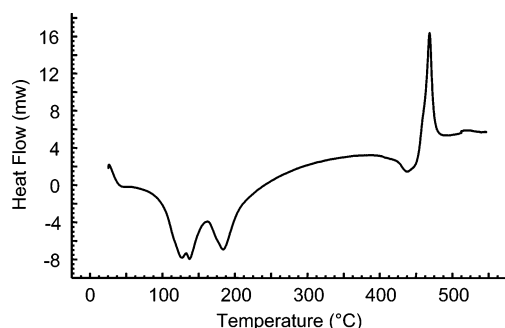
factors and anomalous dispersion corrections were taken from *International Tables for X-ray Crystallography*.<sup>23</sup> Structure solution, refinement, and generation of publication materials were performed using SHELXTL v6.12 software. Additional details are given in Table 1, and a thermal ellipsoid plot (at the 50% probability level) is given in Figure 1B.

**Catalysis.** Complex **1Mn** (0.01 mmol) was dissolved in a solution of 1.0 mmol methyltricaprylammonium chloride in 50 mL of 1,2-dichloroethane, and the precipitated NaCl was filtered off. In a typical reaction, the alkene substrate (1.0 mmol), 1 mL of the POM stock solution (containing 0.2 μmol of **1Mn**), and 3 μL of decane were stirred at 25 °C under Ar in a sealed vial. The reaction was initiated by the addition of 68 μL of 30% aqueous H<sub>2</sub>O<sub>2</sub> (0.002 mol). The organic products were identified and quantified by GC using decane as the internal standard. The final H<sub>2</sub>O<sub>2</sub> concentration was determined by standard iodometric analyses.<sup>24</sup>

## Results and Discussion

**Synthesis and Physical Properties.** Complexes **1Mn** and **1Co** are isolated as decomposition products from a solution of the pure K<sup>+</sup> salts of [(Mn(OH<sub>2</sub>)<sub>2</sub>)<sub>3</sub>(A-α-PW<sub>9</sub>O<sub>34</sub>)<sub>2</sub>]<sup>12-</sup> and [(Co(OH<sub>2</sub>)<sub>2</sub>)<sub>3</sub>(A-α-PW<sub>9</sub>O<sub>34</sub>)<sub>2</sub>]<sup>12-</sup> in 0.5 M NaCl at 25 °C. Both products crystallize by slow evaporation over a period of 3 to 5 days and are obtained in modest yield. Nadjo and Kortz have recently reported the structurally analogous Ni-containing complexes [Ni<sub>6</sub>As<sub>3</sub>W<sub>24</sub>O<sub>94</sub>(H<sub>2</sub>O)<sub>2</sub>]<sup>17-</sup> and [Ni<sub>4</sub>Mn<sub>2</sub>P<sub>3</sub>W<sub>24</sub>O<sub>94</sub>(H<sub>2</sub>O)<sub>2</sub>]<sup>17-</sup>.<sup>25</sup> However, these complexes were not isolated through the decomposition of the A-type sandwich complex [(Ni(OH<sub>2</sub>)<sub>2</sub>)<sub>3</sub>(A-α-XW<sub>9</sub>O<sub>34</sub>)<sub>2</sub>]<sup>12-</sup> (where X = P(V) or As(V)), but instead as a byproduct of the synthesis of the B-type [Ni<sub>3</sub>Na(H<sub>2</sub>O)<sub>2</sub>(AsW<sub>9</sub>O<sub>34</sub>)<sub>2</sub>]<sup>11-</sup> sandwich. The Ni<sub>6</sub> complex takes several months to crystallize in 8% yield.

The FT-IR spectra of polyanions **1Mn** and **1Co** are shown in Figure 2. The spectra of **1Mn** and **1Co** are comparable to those of their parent complexes [(M(OH<sub>2</sub>)<sub>2</sub>)<sub>3</sub>(A-α-PW<sub>9</sub>O<sub>34</sub>)<sub>2</sub>]<sup>12-</sup> (where M = Mn(II) or Co(II)) in that they exhibit similar terminal W–O stretching and W–O–W bridging frequen-

**Figure 2.** Infrared spectra of (A) [(Mn(OH<sub>2</sub>)Mn<sup>12</sup>PW<sub>9</sub>O<sub>34</sub>)<sub>2</sub>(PW<sub>6</sub>O<sub>26</sub>)]<sup>17-</sup>, **1Mn**, and (B) [(Co(OH<sub>2</sub>)Co<sup>12</sup>PW<sub>9</sub>O<sub>34</sub>)<sub>2</sub>(PW<sub>6</sub>O<sub>26</sub>)]<sup>17-</sup>, **1Co**.**Figure 3.** Differential scanning calorimetry (DSC) curve for **1Mn** from 20 °C to 550 °C at a rate of 20 °C/min.

cies.<sup>26</sup> Each complex displays subtle differences in the intensities of these bands. Differences in the splitting of the  $\nu_3$  vibrational mode of the PO<sub>4</sub> units are seen for **1Mn** relative to **1Co**. Most likely a combination of two factors is responsible. First, **1Mn** and **1Co** contain two different types of phosphate groups by symmetry. Second, Jahn–Teller effects present for high spin Co(II), but not for high spin Mn(II), may also be responsible for changes in the splitting of the  $\nu_3$  mode of the PO<sub>4</sub> bands. Similar observations have been made for the analogous B-type Keggin sandwich family where the Jahn–Teller distorted [(Cu(OH<sub>2</sub>)<sub>2</sub>Cu<sub>2</sub>(PW<sub>9</sub>O<sub>34</sub>)<sub>2</sub>)]<sup>10-</sup> shows complete splitting of the  $\nu_3$  vibrational mode into two well resolved bands, while the nondistorted [(Zn(OH<sub>2</sub>)<sub>2</sub>Zn<sub>2</sub>(PW<sub>9</sub>O<sub>34</sub>)<sub>2</sub>)]<sup>10-</sup> exhibits only one band for the same PO<sub>4</sub> unit.<sup>27</sup>

The thermal behavior of **1Mn** and **1Co** is consistent with their molecular formulas, analytical data, and crystal structures.<sup>28,29</sup> Their differential scanning calorimetry (DSC) curves show two endothermic and one exothermic processes in the region from 20 °C to 550 °C (Figure 3). The peaks in the first endothermic process (from 83 °C to 217 °C) are

- (23) *International Tables for X-ray Crystallography*; Kynoch Academic Publishers: Dordrecht, Netherlands, 1992; Vol. C.  
 (24) Day, R. A.; Underwood, A. L. *Quantitative Analysis*, 5th ed.; Prentice Hall: Englewood Cliffs, NJ, 1986.  
 (25) Mbomekalle, I. M.; Keita, B.; Nierlich, M.; Kortz, U.; Berthet, P.; Nadjo, L. *Inorg. Chem.* **2003**, *42*, 5143–5152.

- (26) (a) Rocchiccioli-Deltcheff, C.; Thouvenot, R. *J. Chem. Res., Synop.* **1977**, *2*, 46–47. (b) Rocchiccioli-Deltcheff, C.; Fournier, M.; Franck, R.; Thouvenot, R. *Inorg. Chem.* **1983**, *22*, 207–216. (c) Thouvenot, R.; Fournier, M.; Franck, R.; Rocchiccioli-Deltcheff, C. *Inorg. Chem.* **1984**, *23*, 598–605.  
 (27) Randall, W. J.; Droege, M. W.; Mizuno, N.; Nomiya, K.; Weakley, T. J. R.; Finke, R. G. In *Inorganic Syntheses*; Cowley, A. H., Ed.; John Wiley and Sons: New York, 1997; Vol. 31, pp 167–185.  
 (28) Wendlandt, W. W. *Thermal Analysis*; Wiley-Interscience: New York, 1986.  
 (29) Representative papers on thermal analysis of POMs: (a) Aboul-Gheit, A. K.; Summan, A.-H. M. *Thermochim. Acta* **1989**, *140*, 21–29. (b) Varga, M.; Török, B.; Molnár, Á. *J. Therm. Anal.* **1998**, *53*, 207–215. (c) Cindrić, M.; Strukan, N.; Vrdoljak, V.; Devčić, M.; Kamenar, B. *J. Coord. Chem.* **2002**, *55*, 705–710. (d) Dillon, C. J.; Holles, J. H.; Davis, R. J.; Labinger, J. A.; Davis, M. E. *J. Catal.* **2003**, *218*, 54–66.

**Table 2.** Selected Bond Lengths (Å) and Angles (deg) for **1Mn**

W(1)–O(1)	1.692(9)
W(3)–O(27)	1.905(9)
P(1)–O(46)	1.533(9)
Mn(3)–O(75)	2.099(9)
W(1)–O(27)–W(3)	153.1(5)
P(1)–O(46)–Mn(3)	123.9(5)
Mn(3)–O(75)–W(19)	134.3(5)

attributed to the desorption of waters of crystallization from the lattice structure. The second process (from 425 °C to 442 °C) is most likely the loss of the two coordinated H<sub>2</sub>O molecules on **1Mn** (Figure 1B). However, thermogravimetric analysis (TGA) does not exhibit the high sensitivity necessary for the quantification of this stepwise dehydration. Finally, there is an exothermic peak (from 442 °C to 475 °C) that is attributable to the decomposition of the complex. This is corroborated by FT-IR data which show significant changes in the W–O stretching and W–O–W bending modes after heating to 550 °C.<sup>26</sup>

The UV–visible spectrum of **1Mn** is not structurally informative because the Mn-centered d–d transitions are obscured by the intense charge-transfer bands (tungsten-to-oxygen) exhibited by POMs. Complex **1Co**, however, exhibits a Co-centered d–d transition at 560 nm ( $\epsilon = 416 \text{ M}^{-1} \text{ cm}^{-1}$ ) as well as the characteristic charge-transfer bands. This band is shifted to a higher wavelength from that of the parent complex, [(Co(OH<sub>2</sub>)<sub>2</sub>)<sub>3</sub>(A- $\alpha$ -PW<sub>9</sub>O<sub>34</sub>)<sub>2</sub>]<sup>12-</sup> (536 nm,  $\epsilon = 64 \text{ M}^{-1} \text{ cm}^{-1}$ ).<sup>16</sup> The substantial magnetic moments of **1Mn** and **1Co** ( $\mu_{\text{eff}} = 11.68$  and  $12.69 \mu_{\text{B}}/\text{mol}$ , respectively) preclude the acquisition of <sup>31</sup>P NMR.

**Solid State Characterization.** The X-ray crystal structure of **1Mn** is shown in Figure 1 in polyhedral and ball-and-stick notation. Polyanion **1Mn** consists of two (Mn<sup>II</sup>OH<sub>2</sub>)-Mn<sup>II</sup>PW<sub>9</sub>O<sub>34</sub><sup>3-</sup> Keggin units connected by a PW<sub>6</sub>O<sub>26</sub><sup>11-</sup> fragment to form a C-shaped structure. Bond valence sum calculations on **1Mn** yield an average oxidation state of  $2.2 \pm 0.1$  for Mn.<sup>30</sup> Selected bond lengths and angles for **1Mn** are given in Table 2. Infrared and elemental analysis data are consistent with the structure determined by X-ray crystallography (Figure 2).

A combination of two key structural features makes **1Mn** unique. First, the (Mn<sup>II</sup>OH<sub>2</sub>)-Mn<sup>II</sup>PW<sub>9</sub>O<sub>34</sub><sup>3-</sup> Keggin unit is interesting in that it exhibits the uncommon structural property of a B- $\alpha$ -junction at the site of metal incorporation (Figure 4A). This type of junction was first reported by Weakley and has only been seen in a few additional POMs.<sup>31–34</sup> In contrast, a B- $\beta$ -junction has been seen at the site of metal incorporation in several sandwich-type POMs (Figure 4B).<sup>33,35–38</sup> This prevalence (and the presumed stability) of a  $\beta$ -junction over an  $\alpha$ -junction in sandwich-type POMs is in direct contrast to the known relative

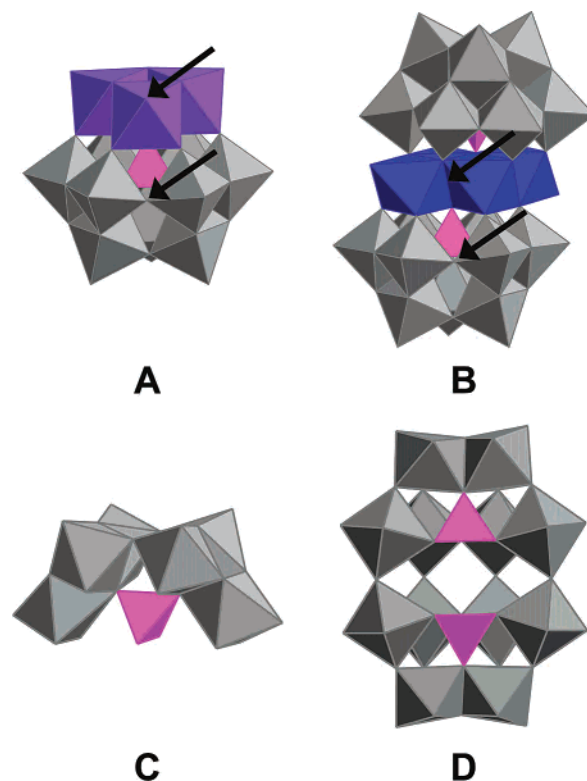


**Figure 4.** (A) Polyhedral representation of one (Mn<sup>II</sup>OH<sub>2</sub>)Mn<sup>II</sup><sub>2</sub>PW<sub>9</sub>O<sub>34</sub><sup>3-</sup> unit showing the B- $\alpha$ -junction at the site of metal incorporation. The arrows show the corner–corner alignment characteristic of the  $\alpha$  isomer. (B) The sandwich-type POM K<sub>10</sub>[(Co(OH<sub>2</sub>)<sub>2</sub>Co<sub>2</sub>(PW<sub>9</sub>O<sub>34</sub>)<sub>2</sub>)]<sup>12-</sup> exhibits a B- $\beta$ -junction at the site of metal incorporation. The arrows show the corner–edge alignment characteristic of the  $\beta$  isomer. (C) Polyhedral notation of the unique B-type hexavacant unit PW<sub>6</sub>O<sub>26</sub><sup>11-</sup> that bridges the two (Mn<sup>II</sup>OH<sub>2</sub>)-Mn<sup>II</sup><sub>2</sub>PW<sub>9</sub>O<sub>34</sub><sup>3-</sup> units of **1Mn**. (D) The hexavacant Wells–Dawson anion [H<sub>2</sub>P<sub>2</sub>W<sub>12</sub>O<sub>48</sub>]<sup>12-</sup> can be thought of as the association of two A-type PW<sub>6</sub>O<sub>26</sub><sup>11-</sup> units.

thermodynamic stabilities exhibited by the  $\alpha$  and  $\beta$  isomers (i.e. Baker–Figgis isomers) of the parent Keggin structure.<sup>39</sup> The most likely explanation for the prevalence of B- $\beta$ -junctions in sandwich-type POMs is that the repulsion present between the coordinated water ligands of the external metal sites and the bridging oxygen atoms of the neighboring belt tungstens in each of the [XW<sub>9</sub>O<sub>34</sub>]<sup>n-</sup> units dominates over the small energetic differences between the Baker–Figgis isomers.<sup>36,40</sup> The second unique structural feature of **1Mn** is that the PW<sub>6</sub>O<sub>26</sub><sup>11-</sup> fragment is a B-type hexavacant Keggin (Figure 4C). The hexavacant Wells–Dawson analogues [H<sub>2</sub>P<sub>2</sub>W<sub>12</sub>O<sub>48</sub>]<sup>12-</sup> and [H<sub>2</sub>As<sub>2</sub>W<sub>12</sub>O<sub>48</sub>]<sup>12-</sup> and their derivatives have been known for some time (Figure 4D).<sup>41–43</sup> These

(30) Brown, I. D.; Altermatt, D. *Acta Crystallogr., Sect. B* **1985**, 244–247.

(31) Weakley, T. J. R. *J. Chem. Soc., Chem. Commun.* **1984**, 1406–1407.

(32) Gómez-García, C. J.; Coronado, E.; Ouahab, L. *Angew. Chem., Int. Ed. Engl.* **1992**, 31, 649–651.

(33) Clemente-Juan, J. M.; Coronado, E.; Galán-Mascarós, J. R.; Gómez-García, C. J. *Inorg. Chem.* **1999**, 38, 55–63.

(34) Kortz, U.; Mbomekalle, I. M.; Keita, B.; Nadjo, L.; Berthet, P. *Inorg. Chem.* **2002**, 41, 6412–6416.

(35) Finke, R. G.; Droege, M. *J. Am. Chem. Soc.* **1981**, 103, 1587–1589.

(36) Finke, R. G.; Droege, M. W.; Domaille, P. J. *Inorg. Chem.* **1987**, 26, 3886–3896.

(37) Gómez-García, C. J.; Coronado, E.; Gómez-Romero, P.; Casañ-Pastor, N. *Inorg. Chem.* **1993**, 32, 3378–3381.

(38) Alizadeh, M. H.; Razavi, H.; Zonoz, F. M.; Mohammadi, M. R. *Polyhedron* **2003**, 22, 933–939.

(39) (a) Weinstock, I. A.; Cowan, J. J.; Barbuzzi, E. M. G.; Zeng, H.; Hill, C. L. *J. Am. Chem. Soc.* **1999**, 121, 4608–4617. (b) López, X.; Maestre, J. M.; Bo, C.; Poblet, J.-M. *J. Am. Chem. Soc.* **2001**, 123, 9571–9576. (c) Neiwert, W. A.; Cowan, J. J.; Hardcastle, K. I.; Hill, C. L.; Weinstock, I. A. *Inorg. Chem.* **2002**, 41, 6950–6952.

(40) See Figure 5B in: Anderson, T. M.; Zhang, X.; Hardcastle, K. I.; Hill, C. L. *Inorg. Chem.* **2002**, 41, 2477–2488.

(41) Contant, R.; Ciabrini, J. P. *J. Chem. Res., Synop.* **1977**, 222.

(42) Contant, R.; Thouvenot, R. *Can. J. Chem.* **1991**, 69, 1498–1506.

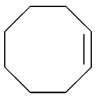
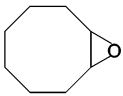
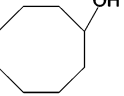
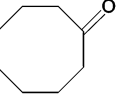
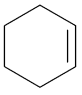
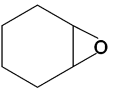
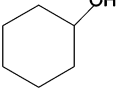
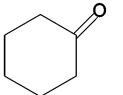
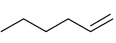
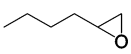
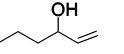
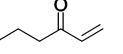
Wells–Dawson anions have alternatively been described as the association of two  $XW_6O_{26}^{11-}$  (where  $X = P(V)$  or  $As(V)$ ) units.<sup>44</sup> However, these hexavacant fragments are A-type, with three  $WO_6$  octahedra having been removed from three different  $W_3O_{13}$  triads in each half of the  $X_2W_{12}O_{48}^{14-}$  polyanions.

To establish that the observed decomposition in 0.5 M NaCl and the isolation of crystals of this new C-shaped POM were not exclusive to Mn(II), a low resolution ( $R_1 = 12.75$ ) X-ray structure of **1Co** was obtained (see SI). The crystals of **1Co** were of significantly poorer quality than those of **1Mn** and could not be face indexed, leading to a poor absorption correction. Nonetheless, the structure of the polyanion unit was established unequivocally, and it is isostructural with **1Mn**.

A similar structural motif to **1Mn** and **1Co** was reported by Coronado et al. for  $[Co_7(H_2O)_2(OH)_2P_2W_{25}O_{94}]^{16-}$  where a Co heteroatom is present in the central unit and the surrounding fragment contains an additional W atom.<sup>45</sup> In addition, the two nickel-containing compounds,  $[Ni_6As_3W_{24}O_{94}(H_2O)_2]^{17-}$  and  $[Ni_4Mn_2P_3W_{24}O_{94}(H_2O)_2]^{17-}$ , recently reported by Nadjo and Kortz are isostructural to the title compounds.<sup>25</sup> Finally, it is noteworthy that a single  $K^+$  cation lies in the bend of **1Mn** and is intimately associated with the POM (Figure 1). However, since a cation is not present in the bend of the Coronado polyanion, the Nadjo/Kortz Ni-containing analogues, or **1Co**, there is clearly no energetic requirement for its presence in this site.

**Catalysis.** The  $H_2O_2$ -based oxidation of three representative alkenes catalyzed by **1Mn** and the distribution of alkene-derived products obtained is reported in Table 3. Manganese-containing POMs of the sandwich-type structural motif are excellent catalysts for the  $H_2O_2$ -based epoxidation of alkenes. Both high selectivity and high turnover numbers can be achieved.<sup>46</sup> Recently, a “substituent effect” was identified where the number of adjacent d-electron containing metals that replace the skeletal  $d^0$  centers (usually W(VI) or Mo(VI)) within the POM framework influenced catalytic activity.<sup>47–53</sup> Neumann and co-workers, however, show that there is decreased catalytic activity when a third or fourth

**Table 3.** Product Distributions for Ambient Temperature Oxidation of Alkenes by  $H_2O_2$  Catalyzed by **1Mn**<sup>a</sup>

Substrate (Catalyst)	Products Selectivity (TON) <sup>b</sup>		
 ( <b>1Mn</b> )	 99% (1852)	 0 <sup>c</sup>	 1% (9)
 ( <b>1Mn</b> )	 94% (172)	 2% (4)	 4% (8)
 ( <b>1Mn</b> )	 99% (20)	 0 <sup>c</sup>	 0 <sup>c</sup>

<sup>a</sup> Conditions: 68  $\mu$ L of 30%  $H_2O_2$  was injected into a vial containing 1 mL of POM stock solution (0.2  $\mu$ mol **1Mn**) and 1.0 mmol alkene substrate under Ar to initiate the reaction. Organic products were identified and quantified by GC/MS and GC. <sup>b</sup> Selectivity = (moles of indicated product/moles of all organic products derived from the substrate)  $\times$  100% (TON = moles of indicated product after 24 h/moles of catalyst). <sup>c</sup> No products within the detection limit ( $<0.2\%$ ).

reactive transition metal (Mn(II) or Co(II)) is substituted into the starting  $[WZnMn_2(ZnW_9O_{34})_2]^{12-}$ .<sup>46a,54</sup> The presence of two sets of three adjacent Mn(II) centers in our POM and their effect on the catalytic activity were therefore of interest. In the case of *cis*-cyclooctene, **1Mn** gives 300 more turnovers over the same period of time than the previously reported  $\alpha\beta\beta\alpha$ - $[(MnOH)_2Mn_2(As_2W_{15}O_{56})_2]^{16-}$  (1550 turnovers) with no adverse effect on selectivity.<sup>55</sup> For cyclohexene, an improvement in selectivity is seen with **1Mn** relative to  $\alpha\beta\beta\alpha$ - $[(MnOH)_2Mn_2(As_2W_{15}O_{56})_2]^{16-}$ . The  $H_2O_2$  efficiency is low in all three reactions, indicating that the complex catalyzes disproportionation.<sup>56</sup> The POM is stable under catalytic conditions with no decomposition products being observed by FT-IR (after 24 h and 1852, 172, and 20 turnovers for *cis*-cyclooctene, cyclohexene, and 1-hexene, respectively).

**Acknowledgment.** We would like to thank the Army Research Office (Grant DAMD17-99-C-9012), the National

- (43) (a) Judd, D. A.; Chen, Q.; Campana, C. F.; Hill, C. L. *J. Am. Chem. Soc.* **1997**, *119*, 5461–5462. (b) Contant, R.; Hervé, G. *Rev. Inorg. Chem.* **2002**, *22*, 63–111.
- (44) Contant, R.; Tézé, A. *Inorg. Chem.* **1985**, *24*, 4610–4614.
- (45) Borrás-Almenar, J. J.; Clemente-Juan, J. M.; Clemente-Leon, M.; Coronado, E.; Galan-Mascaros, J. R.; Gómez-García, C. J. In *Polyoxometalate Chemistry: From Topology via Self-Assembly to Applications*; Pope, M. T., Müller, A., Eds.; Dordrecht: The Netherlands, 2001; p 234.
- (46) Representative catalytic studies of manganese-containing sandwich-type POMs include: (a) Neumann, R.; Gara, M. *J. Am. Chem. Soc.* **1994**, *116*, 5509–5510. (b) Neumann, R.; Gara, M. *J. Am. Chem. Soc.* **1995**, *117*, 5066–5074. (c) Neumann, R.; Khenkin, A. M. *Chem. Commun.* **1998**, 1967–1968. (d) Ben-Daniel, R.; Weiner, L.; Neumann, R. *J. Am. Chem. Soc.* **2002**, *124*, 8788–8789. (e) Adam, W.; Alsters, P. L.; Neumann, R.; Saha-Moller, C. R.; Sloboda-Rozner, D.; Zhang, R. *Synlett* **2002**, 2011–2014.
- (47) Keita, B.; Lu, Y. W.; Nadjo, L.; Contant, R.; Abbessi, M.; Canny, J.; Richet, M. *J. Electroanal. Chem. Interfacial Electrochem.* **1999**, *477*, 146–157.
- (48) Contant, R.; Abbessi, M.; Canny, J.; Richet, M.; Keita, B.; Belhouari, A.; Nadjo, L. *Eur. J. Inorg. Chem.* **2000**, 567–574.
- (49) Contant, R.; Abbessi, M.; Canny, J.; Belhouari, A.; Keita, B.; Nadjo, L. *Inorg. Chem.* **1997**, *36*, 4961–4967.

- (50) Keita, B.; Belhouari, A.; Nadjo, L.; Contant, R. *J. Electroanal. Chem.* **1998**, *442*, 49–57.
- (51) Keita, B.; Girard, F.; Nadjo, L.; Contant, R.; Canny, J.; Richet, M. *J. Electroanal. Chem.* **1999**, *478*, 76–82.
- (52) Belghiche, R.; Contant, R.; Lu, Y. W.; Keita, B.; Abbessi, M.; Nadjo, L.; Mahuteau, J. *Eur. J. Inorg. Chem.* **2002**, 1410–1414.
- (53) Keita, B.; Mbomekalle, I. M.; Nadjo, L.; Contant, R. *Electrochem. Commun.* **2001**, *3*, 267–273.
- (54) For example,  $[WZnMn_2(ZnW_9O_{34})_2]^{12-}$  gives 2300 turnovers in 20 h while the tri-Mn-substituted  $[WMnMn_2(ZnW_9O_{34})_2]^{12-}$  gives only 385 turnovers in the same amount of time. See ref 46a for further catalytic data.
- (55) Mbomekalle, I. M.; Keita, B.; Nadjo, L.; Berthet, P.; Neiwert, W. A.; Hill, C. L.; Ritorto, M. D.; Anderson, T. M. *J. Chem. Soc., Dalton Trans.* **2003**, 2646–2650.
- (56)  $H_2O_2$  efficiency is defined as the number of moles of  $H_2O_2$  remaining after 24 h reaction time plus the total number of moles of oxidation products formed (epoxide + ketone + alcohol) divided by 0.2 initial mol of  $H_2O_2 \times 100\%$ . The  $H_2O_2$  efficiency was 2% for *cis*-cyclooctene and less than 1% for both cyclohexene and 1-hexene.

*Decomposition of A-Type Sandwiches*

Science Foundation (Grant CHE-0236686), Grant CHE-9974864 for funding the D8 X-ray instrument, and Kenneth I. Hardcastle for assistance with X-ray crystallography.

**Note Added after ASAP:** Due to a production error, the version of this paper posted ASAP on December 6, 2003, contained incorrect footnotes 5 and 6. The version posted on December 9, 2003, contains the correct footnotes.

**Supporting Information Available:** Structure determination parameters, crystal and structure refinement data, and atomic coordinates and isotropic displacement parameters for **1Mn** and **1Co** (in CIF form); partial occupancies for Na and solvent water O atoms for **1Mn**; thermal ellipsoid plot for **1Co**. This material is available free of charge via the Internet at <http://pubs.acs.org>.

IC035115T